Journal of Molecular Structure 1036 (2012) 19–27

Contents lists available at SciVerse ScienceDirect

Journal of Molecular Structure

journal homepage: www.elsevier.com/locate/molstruc

Structures of hydrazones, (*E*)-2-(1,3-benzothiazolyl)-NH—N═CH—Ar, [Ar =4-(pyridin-2-yl)phenyl, pyrrol-2-yl, thien-2-yl and furan-2-yl]: Difference in conformations and intermolecular hydrogen bonding

Eric B. Lindgren[a], Julliane D. Yoneda[b], Katia Z. Leal[a,c], Antônio F. Nogueira[d], Thatyana R.A. Vasconcelos[a,d], James L. Wardell[e,f,*], Solange M.S.V. Wardell[g]

[a] *Programa de Pós-Graduação em Química, Instituto de Química, Universidade Federal Fluminense, Outeiro de São João Batista s/n°, 24020-141 Niterói-RJ, Brazil*
[b] *Departamento de Química, Instituto de Ciências Exatas, Universidade Federal Fluminense, Rua Des. Ellis Hermydio Figueira 783, 27213-415 Volta Redonda-RJ, Brazil*
[c] *Departamento de Físico-Química, Instituto de Química, Universidade Federal Fluminense, Outeiro de São João Batista s/n°, 24020-141 Niterói-RJ, Brazil*
[d] *Departamento de Química-Orgânica, Instituto de Química, Universidade Federal Fluminense, Outeiro de São João Batista s/n°, 24020-141 Niterói-RJ, Brazil*
[e] *Centro de Desenvolvimento Tecnológico em Saúde (CDTS), Fundação Oswaldo Cruz (FIOCRUZ), Casa Amarela, Campus de Manguinhos, Av. Brasil 4365, 21040-900 Rio de Janeiro-RJ, Brazil*
[f] *Chemistry Department of Chemistry, University of Aberdeen, Old Aberdeen AB24 3UE, Scotland, United Kingdom*
[g] *CHEMSOL, 1 Harcourt Road, Aberdeen AB15 5NY, Scotland, United Kingdom*

HIGHLIGHTS

- ▶ Crystal structures of (*E*)-2-(1,3-benzothiazolyl)-NH—N═CH—Ar(Het) are reported.
- ▶ Differences in the supramolecular arrangements are observed.
- ▶ Calculated conformations are in agreement with crystallographic findings.

ARTICLE INFO

Article history:
Received 1 September 2012
Received in revised form 21 September 2012
Accepted 24 September 2012
Available online 2 October 2012

Keywords:
Hydrazones
2-Hydrazinyl-1,3-benzothiazoles
Crystal structures
Supramolecular arrangements

ABSTRACT

Structures of hydrazones, (*E*)-2-(1,3-benzothiazolyl)-NH—N═CH—Ar(Ar = pyridine-2-yl (**1**), pyrrol-2-yl (**2**), thien-2-yl (**3**) and furan-2-yl (**4**), prepared from 2-hydrazinyl-1,3-benzothiazole and ArCHO, followed by recrystallisation from alcohol solutions, are reported. No significant intramolecular hydrogen bonds are present in any of the four molecules. Different conformations were found between **2** and **3**, on one hand and for **4**, on the other. Thus for **4**, the oxygen atom of the furanyl ring is on the same side of the molecule as is the sulfur atom of the benzothiazole unit, while in contrast, each of the heteroatoms of the thienyl and pyrrole rings lies on opposite sides to the benzothiazole sulphur atom. In addition to the conformational variations, differences are noted in the connections between molecules. Despite the presence in each case of $N_{(hydrazono)}$—H—$N_{(benzothiazolo)}$ intermolecular hydrogen bonds, molecules of **4** are linked into spiral chains, while molecules of **2** and **3** (and indeed all compounds having Ar = substituted phenyl) form symmetric dimers. Further intermolecular interactions, albeit weaker ones, are found in **2** [C—H··N and N—H··π], **3** [C—H··π] and **4** [π··π], while dimers of **1** remain essentially free. Calculations carried out using the DFT(B3LYP)/6-311++G(d,p) method indicated that the conformations determined by crystallography for **2–4** were the more stable.

1. Introduction

For some time, we have been interested in structures of aryl-NH—N═CH-aryl compounds, especially those having potential biological activities [1]. Most recently, the crystal structures of some 2-(1,3-benzothiazolyl)-NH—N═CH—Ar, compounds, prepared from substituted benzaldehydes and 2-hydrazinyl-1,3-benzothiazole [2] were reported. This followed on from a study by Vasconcelos and co-workers on an evaluation of the *in vitro* anticancer activities of these derivatives against three neoplastic cancer cells, namely HL-60 (leukemia), MDAMB-435 (breast) and HCT-8 (colon) [3,see also 4]. 1,3-Benzothiazole derivatives, in general, possess diverse

---

[*] Corresponding author at: Centro de Desenvolvimento Tecnológico em Saúde (CDTS), Fundação Oswaldo Cruz (FIOCRUZ), Casa Amarela, Campus de Manguinhos, Av. Brasil 4365, 21040-900 Rio de Janeiro-RJ, Brazil. Tel./fax: +55 21 2552 0435.
E-mail address: j.wardell@abdn.ac.uk (J.L. Wardell).

0022-2860/$ - see front matter © 2012 Elsevier B.V. All rights reserved.
http://dx.doi.org/10.1016/j.molstruc.2012.09.058

pharmacological activities [5], including as anti-inflammatory [6], antitumor [7–9], analgesic [10] and antimicrobial [11] agents.

Hydrazone derivatives containing heterocyclic fragments have attracted special attention due to their potential as photochromic devices [12,13], and as recording layers in the range of 350–450 nm [14]. Such hydrazone derivatives have also found use as ligands for extraction of metals from environmental samples [15].

Following on from our report [2] on 2-(1,3-benzothiazolyl)-NH—N═CH—Ar, compounds, where Ar = a substituted phenyl derivative, we now wish to report the structures of four other (*E*)-2-(1,3-benzothiazolyl)-NH—N═CH—Arderivatives, where Ar = 4-(pyridin-2-yl)phenyl (**1**), pyrrol-2-yl) (**2**), thien-2-yl (**3**) and furan-2-yl (**4**), see Fig. 1. The structural and theoretical study of compounds, **1**–**4**, was undertaken to ascertain whether the presence of the additional heteroaryl group led to differences in the supramolecular arrangements.

2. Results and discussion

2.1. Preparation and solution properties

The compounds were synthesised from reactions of arenecarbaldehydes and 2-hydrazinyl-1,3-benzothiazole following a general method [3,16]. Compounds **1** and **4** have been previously reported [17]. Recrystallisations of **1**–**4** were performed from EtOH solutions and in each case the (*E*)-isomer was isolated: as has been reported [18], both (*E*) and (*Z*) isomers of related compounds have been detected in solution.

The NMR spectra of **1**–**4** were run in DMSO-d_6 solution. The δ^1H(NH) values, in the range 11.86–12.28 ppm, indicate significant deshielding, as expected for the involvement of these NH moieties in N—H—N strong hydrogen bonding. B3LYP/6-311++G(d,p) theoretical calculations support this conclusion, but point strongly in all cases to centrosymmetric dimers just as found in the solid state for **1**–**3**, see Section 2.3. Calculated δ^1H(NH) of dimers are in the range 13.75–13.99 ppm, which is in agreement with the experimental results, whereas calculated δ^1H(NH) of monomers are in the range 8.32–8.64 ppm, which is far shielded in relation with experimental values. As also will be discussed in Section 2.3, these N—H—N hydrogen bonds in solid **4** result in the creation of chains rather than centrosymmetric dimers. B3LYP/6-311++G(d,p) calculations indicate that chain formation in **4** is not theoretically favoured and that pairing of molecules to give symmetric dimers provides appreciable stability for all **1**–**4.** Indeed the optimized geometry for chains of **4** has the molecules too far apart from each other, which was somewhat expected, since the calculations has been performed on the gas-phase. Hence, it has to be concluded that solid state effects must over-ride the thermodynamic effects for compound **4**. In an attempt to reproduce these solid state effects, both dimer and chain crystal structures were optimized DFT/PBE method. The obtained energies were almost identical, with an ΔE of 2.07×10^{-5} eV. The closeness of molecules, as observed in the experimental structure, was maintained in the optimized chain structure, which was not observed for the gas-phase simulations, stressing the importance of solid state effects for compound **4**.

2.2. Molecular structures

The atom numbering schemes and atom arrangements for **1**–**4** are shown in Fig. 2. Selected bond geometric parameters are shown in Table 1. Molecules **2**–**4** are very near planar, as shown by the torsional angles and the angles between the aromatic rings. The least overall planar molecule of the four is **1**, due to the pyridine-2-yl ring being rotated out of the plane of the rest of the molecule, see Table 1. The orientation of the pyridine ring in **1** places N(4) in the neighbourhood of H(15), see Fig. 2, however the N(4)—H(15) separation, at 2.56 Å (2.47 Å, calculated), suggests at best only a weak intramolecular hydrogen bond. In **2**, the N(2)—H(4) separation, at 2.67 Å (2.63 Å, calculated), is even longer and confirms the absence of aN(4)—H(4)··N(2) intramolecular hydrogen bond, especially as the N(4)—H(4) bond is better sited to form an intermolecular N(4)—H(4)··π bond with the phenyl moiety of the benzotriazole unit, see later. All in all, no significant intramolecular hydrogen bond appears present in any of the four compounds.

Of interest, the orientation in **4** of the heteroaryl furan moiety, relative to the remainder of the molecule, is different from those in compounds **2** and **3**, see Fig. 2. This has consequences for the allowed intermolecular hydrogen bonds and the supramolecular arrangement, see later.

2.3. Crystal structures

The only strong intermolecular interactions found in each of **1**–**4** are the N(1)—H(1)—N(3) hydrogen bonds, see Table 2a. While in compounds, **1**–**3**, these lead to symmetry related dimers, $R_2^2(8)$, in the case of **4** these lead to spiral C(4) chains [19], see Figs. 3a, 4, 5a and 6a. Symmetric dimer formation was generally found for (*E*)-2-(1,3-benzothiazolyl)-NH—N═CH—Arcompounds (Ar = substituted phenyl group), as previously reported [2]. Thus the situation in **4** appears unique for this series of compounds.

B3LYP/6-311++G(d,p) theoretical calculations indicated that the H(1)—N(3) distances within the N(1)—H(1)—N(3) hydrogen bonds in the symmetric dimers are all *ca*. 1.92 Å in **1–3**, compared to the solid state values determined by X-ray crystallography of 2.10(3), 2.12(2) and 2.17(3) Å.

The strong N(1)—H(1)··N(3) hydrogen bond is the only intermolecular interaction in **1**. The shortest Cg—Cg separation between non-equivalent rings [thienyl and phenyl rings] in adjacent layers is longer at 4.2354(15) Å than the accepted cut-off distance of 4.0 Å.

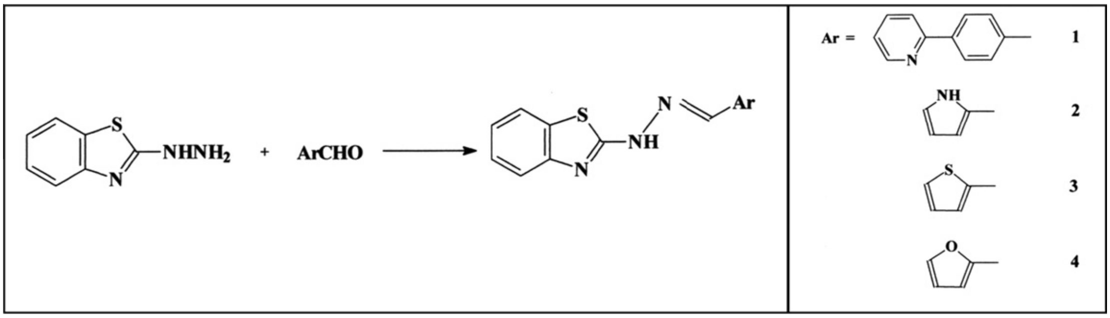

Fig. 1. Formation of compounds **1**–**4**.

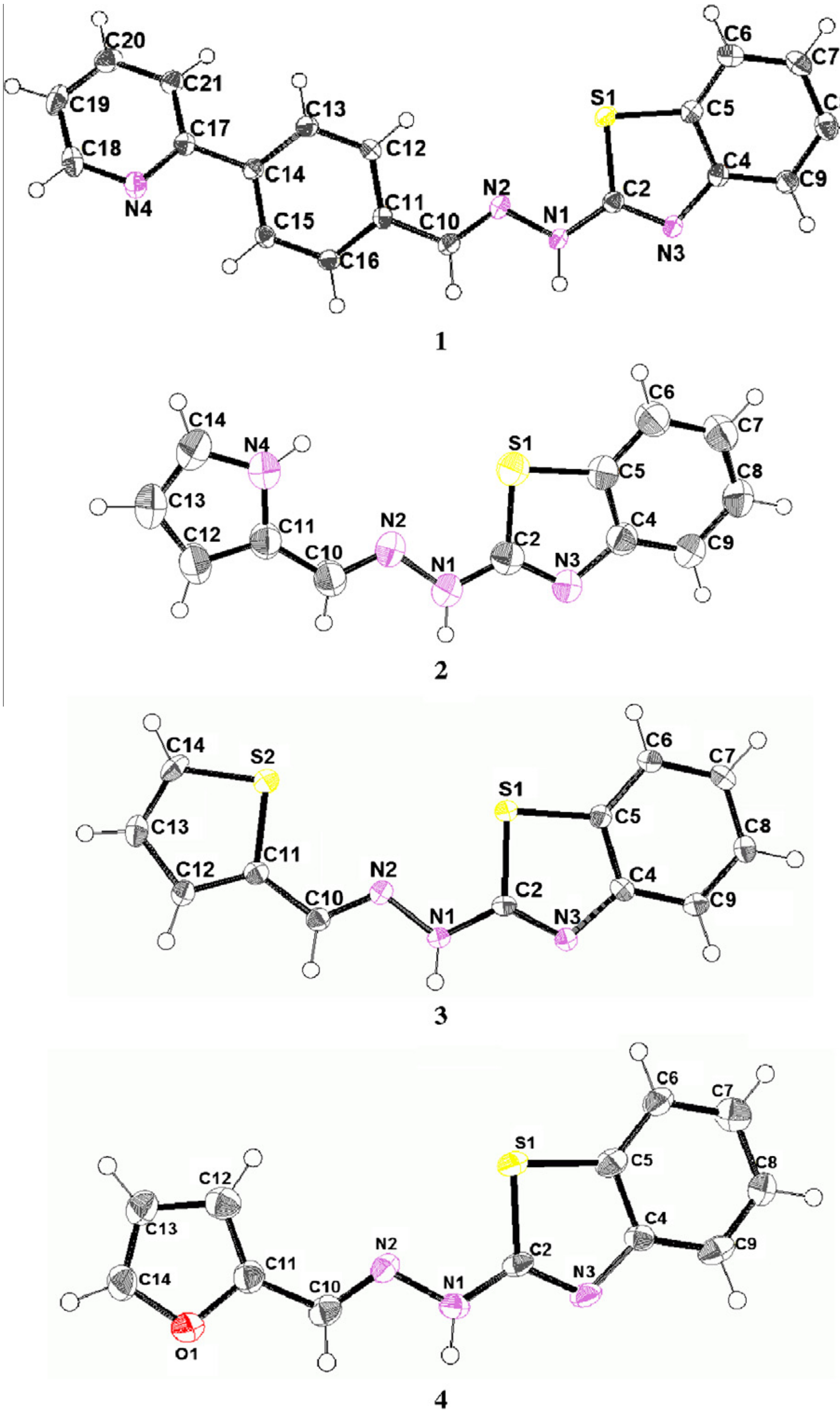

Fig. 2. Atom numbering schemes and arrangements for **1**–**4**. Probability ellipsoids are drawn at the 50% level. Hydrogen atoms are drawn as spheres of arbitrary radius.

In the case of **2**, two short intermolecular contacts, namely H(6)··N(2) and H(4)··$Cg_{(phenyl)}$ at 2.69 Å and 3.31 Å, respectively, between molecules at *x*, *y*, *z* and $-x + 1$, $y - 1/2$, $-z + 1/2$ are present calculated. Both these distances are not individually considered by the PLATON program [20] as being significant. However, the fact that the same pair of molecules are involved in both potential interactions leads us to consider that the C(6)—H(6)··N(2) and N(4)—H(4)··$Cg_{(phenyl)}$ interactions contribute in combination to a positive interaction between the symmetric dimers, generated by the N(1)—H(1)··N(3) hydrogen bonds, see Fig. 4.

The symmetric dimers of **3** are linked by C(7)—H(7)··$\pi_{(thienyl)}$ interactions, see Fig. 5b and Table 2. As shown in Fig. 5b, each dimer is linked to four other dimers, while a combination of N(1)—H(1)··N(3) hydrogen bonds and C(7)—H(7)··$\pi_{(thienyl)}$ hydrogen bonds produces a network of rings made up from six molecules, see Fig. 6c.

As mentioned above, the N(1)—H(1)··N(3) intermolecular interactions in **4** generate chains of molecules, C4,arranged in helices, see Fig. 6a, rather than the symmetric dimers found in **1**–**3**. The helical arrangements, in the direction of the *b* axis, are further

Table 1
Selected geometric parameters (Å, °) for **1**–**4**.

	1		**2**		**3**		**4**	
	X-ray	B3LYP/6-311++G(d,p)	X-ray	B3LYP/6-311++G(d,p)	X-ray	B3LYP/6-311++G(d,p)	X-ray	B3LYP/6-311++G(d,p)
C(2)—N(1)	1.345(3)	1.368	1.324(3)	1.365	1.352(3)	1.368	1.333(9)	1.368
N(1)—N(2)	1.370(3)	1.348	1.382(3)	1.355	1.361(3)	1.349	1.374(8)	1.348
N(2)—C(10)	1.282(3)	1.284	1.269(3)	1.287	1.278(3)	1.285	1.271(9)	1.285
C(10)—C(11)	1.457(3)	1.459	1.439(3)	1.437	1.444(4)	1.442	1.444(10)	1.440
C(2)—N(1)—N(2)	117.6(2)	121.2	113.8(2)	121.1	115.3(2)	121.2	118.3(5)	121.1
N(1)—N(2)—C(10)	115.7(2)	118.1	116.5(2)	118.0	118.2(2)	118.1	115.9(5)	117.9
N(2)—C(10)—C(11)	122.1(2)	122.4	121.8(3)	121.3	119.5(3)	122.3	120.6(6)	121.4
N(3)—C(2)—N(1)—N(2)	176.6(2)	179.9	−180.0(2)	−180.0	−179.9(3)	−180.0	−178.0(7)	−180.0
S(1)—C(2)—N(1)—N(2)	−2.8(3)	−0.1	−0.1(3)	0.0	−0.4(4)	0.0	2.1(9)	0.0
C(2)—N(1)—N(2)—C(10)	−172.5(2)	−179.9	−180.0(2)	−180.0	177.7(3)	180.0	177.4(7)	180.0
N(1)—N(2)—C(10)—C(11)	−179.2(2)	−179.9	179.7(2)	180.0	180.0(3)	180.0	179.5(7)	180.0
N(2)—C(10)—C(11)—C(12)	−3.9(4)	−0.4	−176.6(3)	−180.0	−171.8(3)[a]	−180.0	4.6(14)	0.0
N(2)—C(10)—C(11)—X	175.5(2)[b]	179.8	1.7(4)[c]	0.0	6.9(4)[d]	0.0	−175.8(7)[e]	−180.0
C(10)—C(11)—C(12)—C(13)	179.1(2)	179.8	178.9(3)	180.0	178.2(3)[a]	180.0	−179.4(9)	−180.0
C(15)—C(14)—C(17)—N(4)	23.7(4)	19.9						
C(15)—C(14)—C(17)—C(21)	−156.8(3)	−159.2						

Compound	Angle
Angle between best planes though the aromatic rings	
1	3.77[a]/27.08(8)[b]
2	2.3(2)
3	4.4(2)
4	2.6(5)

[a] C(14) instead of C(12).
[b] X = C(16).
[c] X = N(4).
[d] X = S(2).
[e] X = O(1).

Table 2
Parameters (Å, °) for the intermolecular interactions[a] in **1**–**4**.

Compound	D—H··A	D—H		H··A		D··A		D—H··A	
		X-ray	Theoretical	X-ray	Theoretical	X-ray	Theoretical	X-ray	Theoretical
(a) Intermolecular hydrogen bonds									
1	N(1)—H(1)··N(3$^{\mathrm{i}}$)	0.93(3)	1.059	2.10(3)	1.925	3.020(3)	2.981	171(3)	174.8
2	N(1)—H(1)··N(3$^{\mathrm{ii}}$)	0.88(2)	1.038	2.12(2)	1.934	2.988(3)	2.967	174(2)	173.0
3	N(1)—H(1)··N(3$^{\mathrm{iii}}$)	0.84(3)	1.038	2.17(3)	1.934	2.999(4)	2.968	176(3)	173.3
4	N(1)—H(1)··N(3$^{\mathrm{iv}}$)	0.87(4)	1.038	2.02(4)	1.936	2.889(6)	2.970	178(10)	173.0

Compound	X—Y···Cg	Y···Cg	Y_{perp}	γ	X—Y···Cg	X···Cg
(b) X—Y—π interactions						
2	N(4)—H(4)···Cg(3)	3.31			140	
3	C(7)—H(7)···Cg(2$^{\mathrm{ii}}$)	2.89	2.83	11.41	144	3.697(3)

Compound	Cg(I)··Cg(J)	Cg··Cg	α	β	γ	Cg(I)$_{\mathrm{perp}}$	Cg(J)$_{\mathrm{perp}}$
(c) π··π intermolecular contacts							
4	Cg(1)··Cg(3$^{\mathrm{i}}$)	3.682(4)	1.8(3)	19.42	18.98	3.482(3)	3.472(3)
4	Cg(3)··Cg(1$^{\mathrm{ii}}$)	3.682(4)	1.8(3)	18.98	19.42	3.472(3)	3.481(3)

Symmetry operations: $i = -x, 1 - y, 1 - z$; ii = $1 - x, -1 - y, -z$; iii = $-x, -1 - y, -z$; iv = $1 - x, 1/2 + y, 1/2 - z$.
Cg1 and Cg3 are the centroids of the thiazolyl and phenyl rings, respectively; Alpha is the dihedral angle between the least squares plannes of the overlapping rings. Beta is the angle between the vectors Cg··Cg and Cg(I)$_{\mathrm{perp}}$ where Cg(I)$_{\mathrm{perp}}$ is the perpendicular distance of Cg(I) from the plane of ring J. Similarly γ is the angle between the vectors Cg··Cg and Cg(J)$_{\mathrm{perp}}$. Symmetry codes: (i) $x, 1 + y, z$; (ii) $x, -1 + y, z$.
[a] Cg2 and Cg3 are the centroids of the thiophene and phenyl rings, respectively; γ is the angle at H between the vectors X···Cg and Xperp.: symmetry operations: ii = 1/2 − x, 1/2 + y, −z.

supported by $\pi_{(\mathrm{thiazoly})}\cdot\cdot\pi_{(\mathrm{phenyl})}$ stacking interactions between alternate molecules in the chains, see Fig. 6b. There are no interactions between the chains. Overall, a one-dimension array is present. The packing of the molecules **1**–**4** are shown in Fig. 7.

2.4. Calculations on molecular conformations and hydrogen bonding

Table 3 shows the results of the *ab initio* B3LYP/6-311++G(d,p) calculations. For **2** and **3**, the conformer B is the most stable, whereas the conformer A is the most stable for **4**, confirming the crystallography findings. This type of calculation should be extremely useful in predicting conformational preferences of similar structures since the geometries obtained experimentally by X-ray diffraction and theoretically by molecular modelling are very close (RMS = 0.193 Å for **2**, 0.319 Å **3**, and 0.148 Å for **4**. Fig. 8 shows the relative energy vs. dihedral angle at PM3 level. From the lowest energy conformer, the barrier to rotation in **3** is smaller, compared with the other two molecules. On the other hand, in direction to

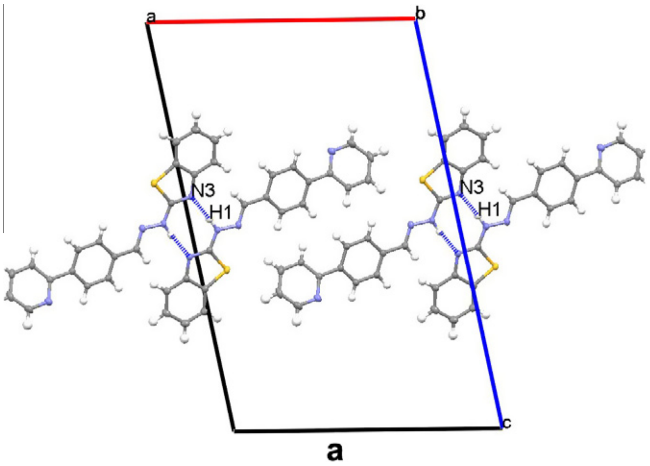

Fig. 3. Compound **1**. (a) Dimers generated by N(1)—H(1)—N(3) hydrogen bonds, symmetry operations are listed in Table 2.

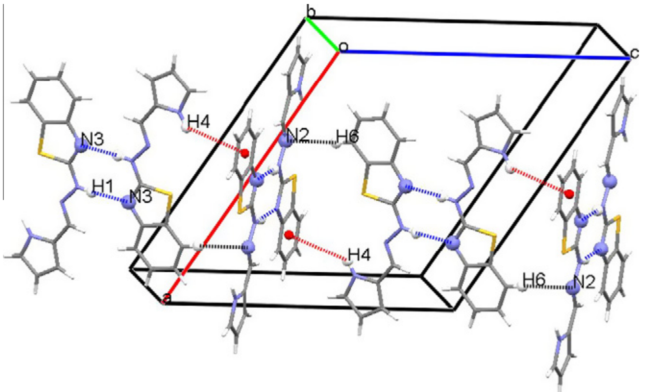

Fig. 4. Dimers of **2**, generated by N(1)—H(1)··N(3) hydrogen bonds [symmetry operations are listed in Table 2], linked by weak C(6)—H(6)··N(2) and N(4)—H(4)···$\pi_{(\text{phenyl})}$ hydrogen bonds [C(6)—H(6)··N(2): d[H(6)··N(2)} = 2.69 Å and [C(6)—H(6)··N(2)] = 133°; N(4)—H(4)···$\pi_{(\text{phenyl})}$: d(H(4)···Cg) = 3.31 Å and N(4)—H(4)·· Cg = 140°).

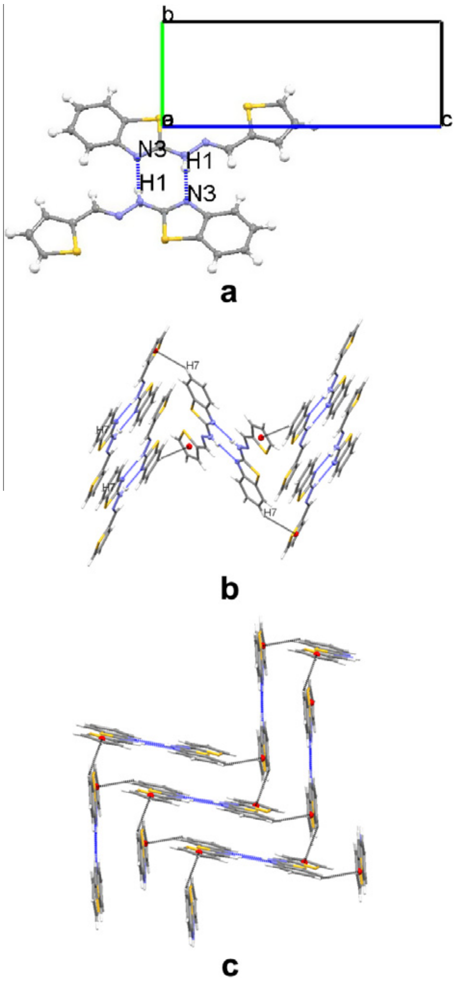

Fig. 5. Compound **3**. (a) Dimers generated from N(1)—H(1)···N(3) hydrogen bonds, shown by blue dashed lines; (b) each dimer is linked by C(7)—H(7)···$\pi_{(\text{thienyl})}$ interactions to four others shown as black dashed lines; (c) the combination of N(1)—H(1)···N(3) hydrogen bonds and C(7)—H(7)···$\pi_{(\text{thienyl})}$ interactions produces a network of rings made up from six molecules. Symmetry operations are listed in Table 2.

the lowest energy conformer, the barrier to rotation in **4** is the smallest.

Despite differences in energies between conformers A and B of each molecule, the semiempirical results are in agreement with the *ab initio* calculations regarding the most stables conformations.

3. Experimental

3.1. General

Melting points were determined on a Fisher-Johns apparatus and are uncorrected. Infrared spectra were recorded on a Perkin–Elmer 1420 spectrometer in KBr. Mass spectra (ESI-MS) were recorded on a ZQ single quadrupole mass spectrometer. NMR spectra were recorded on a Varian Unity Plus 300 spectrometer operating at 300.00 MHz (^{1}H) and 75.0 MHz (^{13}C) in DMSO-d$_6$ solutions.

3.2. Synthesis

1,3-Benzothiazole hydrazoneswere prepared from reactions between 2-hydrazinobenzothiazole(1 mmol) and heteroaromatic aldehydes(1 mmol) in ethanol (10 ml) at room temperature. The progress of the reactions were monitored by thin-layer chromatography on F254 silica-gel pre-coated sheets (Merck), using chloroform/methanol mixture as eluent, and visualized under UV light. After reaction was complete, the solid product was collected and washed successively with cold alcohol and ethyl ether. For the structure determinations, the samples were recrystallized from EtOH solutions.

Compound 1: (*E*)-2-(2-(4-(pyridin-2-yl)benzylidene)hydrazinyl)benzo[*d*]thiazole.

Yield: 65%; **m.p.**: 258–260 °C. **ESI-MS**: *m*/*z*[M−H]$^-$: 329.3.

^{1}H NMR [300.00 MHz, DMSO-*d*$_6$]δ: 12.28 (1H; s; NH); 8.69 (1H; d; *J* = 4.5 Hz; H$_{3''}$); 8.20 (1H; s; N=C—H); 8.18 (2H; d; *J* = 8.4 Hz; H$_{3'}$ and H$_{5'}$); 8.00 (1H; d; *J* = 7.8 Hz; H$_4$ or H$_7$); 7.88 (1H; ddd; *J* = 8.1, 7.8 and 2.1 Hz; H$_5$ or H$_6$); 7.81 (2H; d; *J* = 8.4 Hz; H$_{2'}$ and H$_{6'}$); 7.77 (1H; s; H$_{6''}$); 7.46 (1H; d; *J* = 7.5 Hz; H$_7$ or H$_4$); 7.38–7.28 (2H; m; H$_{4''}$ and H$_{5''}$); 7.12 (1H; dd; *J* = 7.8 and 7.5 Hz; H$_6$ or H$_5$) ppm.

^{13}C NMR [75.0 MHz, DMSO-*d*$_6$]δ: 167.2; 155.3; 149.7; 139.5; 137.3; 135.0; 127.0; 126.0; 122.9; 121.7; 121.6; 120.4 ppm.

IR (cm^{-1}; KBr pellets): $\nu_{\max}$ 3427 (NH); 1624 (C=N).

Compound 2: (*E*)-2-(2-((1*H*-pyrrol-2-yl)methylene)hydrazinyl)benzo[*d*]thiazole.

Yield: 62%; **m.p.**: 208–209 °C. **ESI-MS**: *m*/*z*[M−H]$^-$: 241.3.

^{1}H NMR [300.00 MHz, DMSO-*d*$_6$]δ: 11.86 (1H; s; NH); 11.26 (1H; s; NH); 7.97 (1H; s; N=C—H); 7.71 (1H; d; *J* = 7.5 Hz; H$_4$ or

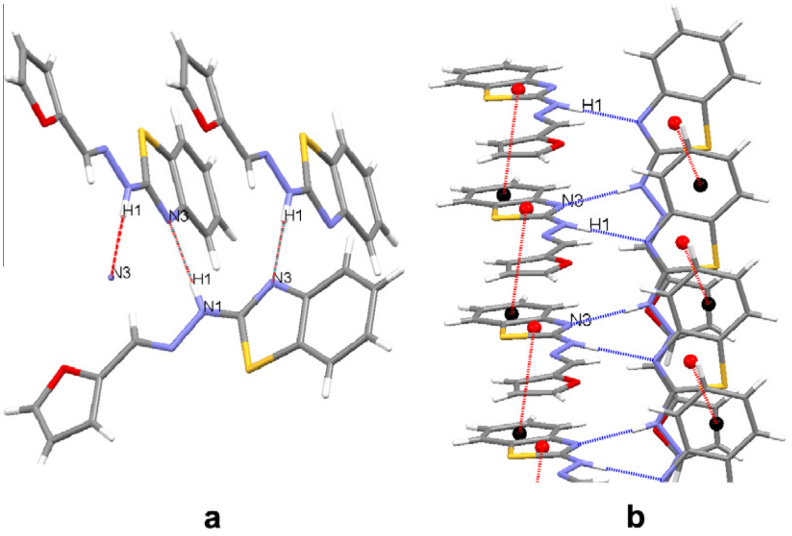

Fig. 6. Compound **4**. (a) A partial helical chain, **C4**, of molecules generated from N(1)—H(1)···N(3) hydrogen bonds n the direction of the *b* axis, shown by dashed lines; (b) alternate molecules in the helical chains are linked by $\pi_{(\text{thiazoly})}\cdots\pi_{(\text{phenyl})}$ stacking interactions. Symmetry operations are listed in Table 2.

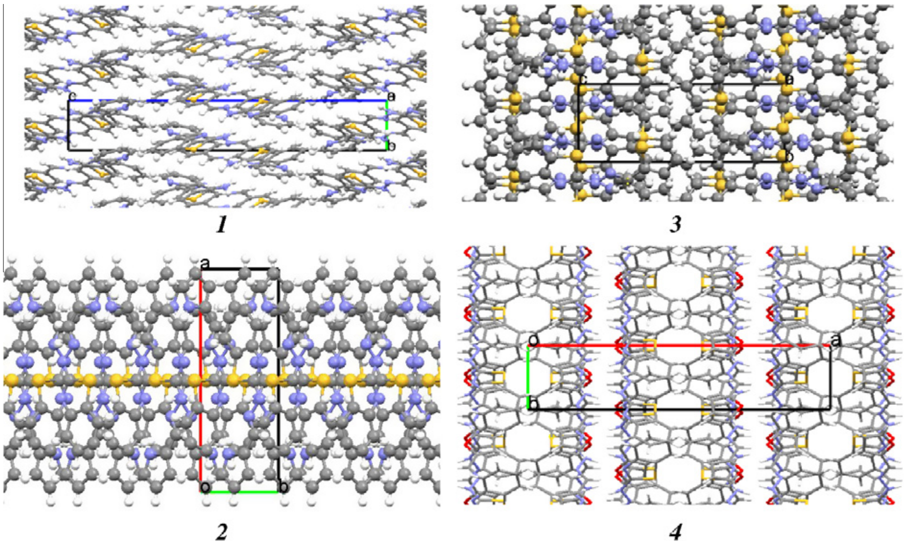

Fig. 7. Packing diagrams for compounds **1–4**.

H_7); 7.36 (1H; d; *J* = 7.2 Hz; H_7 or H_4); 7.25 (1H; dd; *J* = 8.1 and 7.2 Hz; H_5 or H_6); 7.05 (1H; dd; *J* = 7.8 and 7.2 Hz; H_6 or H_5); 6.91 (1H; d; *J* = 1.5 Hz; $H_{5'}$); 6.44 (1H; s; H'_4); 6.13 (1H; dd; *J* = 5.4 and 2.4 Hz; $H_{3'}$) ppm.

^{13}C NMR [75.0 MHz, DMSO-*d*$_6$]δ: 166.4; 137.7; 129.2; 127.3; 125.9; 122.0; 121.4; 121.2; 117.1; 111.9; 109.4 ppm.

IR (cm^{-1}; KBr pellets): ν_{max} 3441 (NH); 1627 (C═N).

Compound 3: (*E*)-2-(2-(thiophen-2-ylmethylene)hydrazinyl) benzo[*d*]thiazole.

(E)-2-Benzothiazolylhydrazone 2-thiophenecarboxaldehyde.

Yield: 60%; **m.p.**: 217–219 °C. **ESI-MS**: *m*/*z*[M−H]$^-$: 258.2.

^{1}H NMR [300.00 MHz, DMSO-*d*$_6$]δ: 12.01 (1H; s; NH); 8.32 (1H; s; N═C—H); 7.71 (1H; d; *J* = 7.8 Hz; H_4 or H_7); 7.58 (1H; d; *J* = 5.1 Hz; $H_{5'}$); 7.38–7.35 (2H; m; $H_{3'}$ and H_7 or H_4); 7.27 (1H; ddd; *J* = 7.8, 7.2 and 1.2 Hz; H_5 or H_6); 7.12–7.05 (2H; m; $H_{4'}$ and H_6 or H_5) ppm.

^{13}C NMR ^{13}C[75.0 MHz, DMSO-*d*$_6$]δ: 166.7; 140.0; 139.3; 129.9; 128.2; 127.8; 125.9; 121.7; 121.6; 117.0 ppm.

IR (cm^{-1}; KBr pellets): ν_{max} 3430 (NH); 1619 (C═N).

Compound 4: (*E*)-2-(2-(furan-2-ylmethylene)hydrazinyl)benzo[*d*]thiazole.

Yield: 68%; **m.p.**: 197–199 °C. **ESI-MS**: *m*/*z*[M−H]$^-$: 242.3.

^{1}H NMR [300.00 MHz, DMSO-*d*$_6$]δ: 12.16 (1H; s; NH); 8.02 (1H; s; N═C—H); 7.80 (1H; d; *J* = 1.8 Hz; $H_{3'}$);7.72 (1H; d; *J* = 7.5 Hz; H_4 or H_7); 7.40 (1H; d; *J* = 7.2 Hz; H_7 or H_4); 7.28 (1H; dd; *J* = 8.1 and 7.2 Hz; H_5 or H_6); 7.09 (1H; dd; *J* = 7.8 and 7.2 Hz; H_6 or H_5); 6.83 (1H; d; *J* = 3.3 Hz; $H_{4'}$); 6.61 (1H; dd; *J* = 3.3 and 2.1 Hz; $H_{5'}$) ppm.

^{13}C NMR [75.0 MHz, DMSO-*d*$_6$]δ: 166.8; 149.6; 144.8; 134.8; 128.8; 126.2; 121.6; 113.0; 112.4 ppm.

IR (cm^{-1}; KBr pellets): ν_{max} 3436 (NH); 1615 (C═N).

3.3. Crystallography

Data for **1–4** were obtained at 120(2) K with Mo Kα radiation by means of the Bruker-Nonius 95 mm CCD camera kappa-goniostate of the EPSRC crystallographic service, based at the University of Southampton. Data collection was carried out under the control of the program COLLECT [21] and data reduction and unit cell

Table 3
ZPE corrected energy (kcal/mol) of each conformer and ΔE between the two conformers, calculated at the B3LYP/6-311++G(d,p) level.

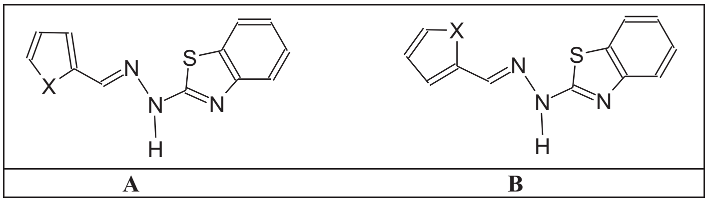

	2		3		4	
	CONFORMER					
	A	B	A	B	A	B
Energy	−678002.06	−678005.71	−893147.87	−893149.22	−690471.53	−690470.90
ΔE (B—A)	−3.65		−1.35		0.63	

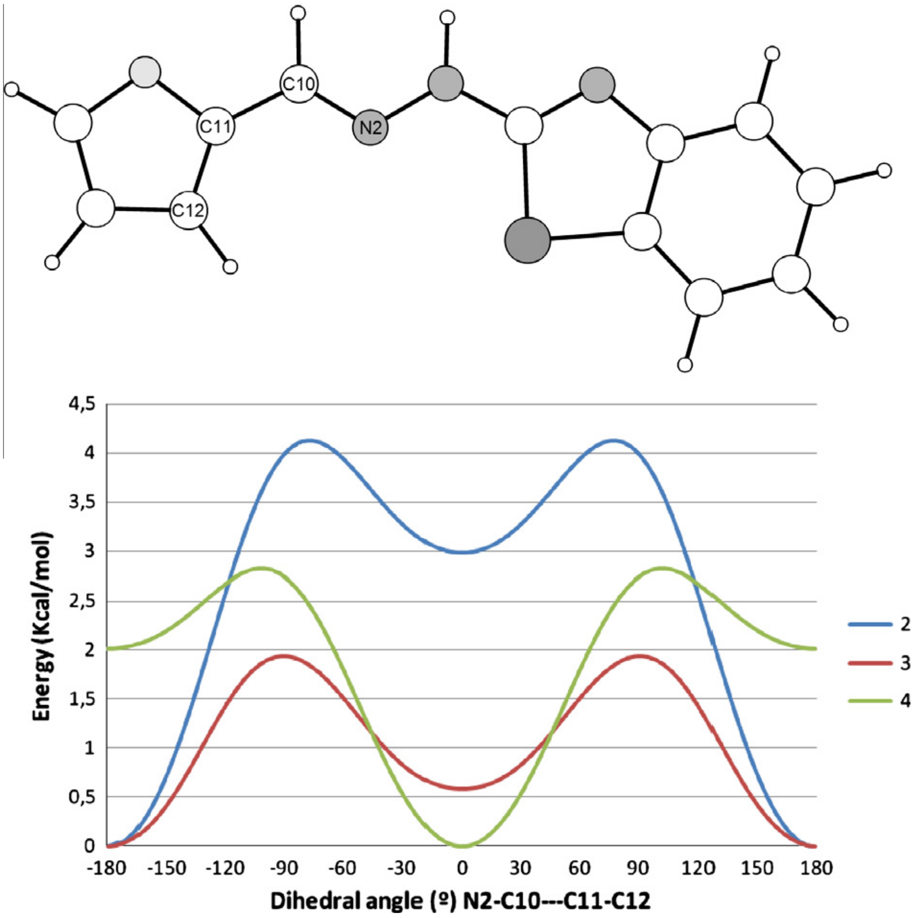

Fig. 8. Graph of relative energy vs. dihedral angle.

refinement were achieved with the COLLECT and DENZO [22] programs. Correction for absorption was achieved in each case by a semi-empirical method based upon the variation of equivalent reflections with the program SADABS [23]. The programs ORTEP-3 for Windows [24] and MERCURY [25] were used in the preparation of the figures. SHELXL97 [26] and PLATON [20] were used in the calculation of molecular geometry. The structures were solved by direct methods using SHELXS-97 [26] and fully refined by means of the program SHELXL-97 [26]. Difference map peaks provided positions for the hydrogen atoms of the NH groups for which the coordinates, along with isotropic displacement parameters, were fully refined. All other hydrogen atoms were placed in calculated positions. Crystal data and structure refinement details are listed in Table 4.

3.4. Calculations

The calculations were performed using the Gaussian 03W program [27]. Molecular geometries of the dimers and the conformers A and B of each monomer were fully optimized using the B3LYP/6-311++G(d,p) level of theory. The zero-point energy correction was applied to the obtained electronic energies. Since no imaginary

Table 4
Crystal data and structure refinement.

	1	**2**	**3**	**4**
Empirical formula	$C_{19}H_{14}N_4S$	$C_{12}H_{10}N_4S$	$C_{12}H_9N_3S_2$	$C_{12}H_9N_3OS$
Formula weight	330.4	242.3	259.34	243.28
Temperature (K)	120(2)		120(2)	120(2)
Wavelength (Å)	0.71073	0.71073	0.71073	0.71073
Crystal system, space group	Monoclinic, *P*21/*n*	Monoclinic, *P*21/*c*	Monoclinic, *P*21/*a*	Monoclinic, *I*2/*a*
Unit cell dimensions:				
a (Å)	16.1124(6)	15.9740(7)	15.4451(5)	21.773(4)
b (Å)	3.8329(2)	4.9329(2)	5.2707(2)	4.6227(7)
c (Å)	25.1692(11)	16.2227(9)	15.7305(5)	28.001(5)
α (°)	90	90	90	90
β (°)	101.272(2)	118.102(2)	116.813(2)	101.082(6)
γ (°)	90	90	90	90
Volume (Å^3)	1524.40(12)	1127.62(9)	1142.88(7)	2200.9(6)
Z, calculated density (Mg/m^3)	4, 1.440	4, 1.427	4, 1.507	8, 1.468
Absorpt. coefficient (mm^{-1})	0.22	0.268	0.443	0.279
F(000)	688	504	536	1008
Crystal size (mm)	0.2 × 0.05 × 0.03	0.36 × 0.18 × 0.06	0.11 × 0.05 × 0.02	0.28 × 0.03 × 0.01
Theta range for data collection (°)	3.01–27.62	3.75–27.49	2.90–27.63	2.91–25.00
Index ranges	$-20 \leqslant h \leqslant 20$	$-20 \leqslant h \leqslant 20$	$-20 \leqslant h \leqslant 19$	$-25 \leqslant h \leqslant 24$
	$-4 \leqslant k \leqslant 4$	$-6 \leqslant k \leqslant 6$	$-6 \leqslant k \leqslant 6$	$-5 \leqslant k \leqslant 5$
	$-32 \leqslant l \leqslant 32$	$-21 \leqslant l \leqslant 20$	$-20 \leqslant l \leqslant 20$	$-26 \leqslant l \leqslant 26$
Reflections collected/unique	13,960	11,498	12,536	5635
Independent reflections	3465	2589	2632	1878
	[*R*(int) = 0.0489]	[*R*(int) = 0.0596]	[*R*(int) = 0.0549]	[*R*(int) = 0.0879]
Reflections observed [$I > 2\sigma(I)$]	2746	1778	2144	1209
Data completion	0.985	0.997	0.989	0.964
Max. and min. transmission			0.9912 and 0.9529	0.9972 and 0.5346
Refinement method	Full-matrix least-squares on F^2	Full-matrix least-squares on F^2	Full-matrix least-squares on F^2	Full-matrix least-squares on F^2
Data/restraints/parameters	3465/0/223	2589/4/164	2632/0/160	1878/1/157
Goodness-of-fit on F^2	1.105	1.031	1.095	1.085
Final *R* indices [$I > 2\sigma(I)$]	$R_1 = 0.058$	$R_1 = 0.052$	$R_1 = 0.050$	$R_1 = 0.098$
	$wR_2 = 0.108$	$wR_2 = 0.120$	$wR_2 = 0.098$	$wR_2 = 0.174$
R indices (all data)	$R_1 = 0.079$	$R_1 = 0.0859$	$R_1 = 0.069$	$R_1 = 0.158$
	$wR_2 = 0.120$	$wR_2 = 0.1381$	$wR_2 = 0.109$	$wR_2 = 0.206$
Largest diff. peak and hole (e/Å^3)	0.282 and −0.321	0.368 and −0.292	0.468 and −0.343	0.490 and −0.400

frequency was found, all the optimized structures were characterized as minima.

Theoretical NMR chemical shifts were calculated using the GIAO B3LYP/6-311++G(d,p) level of theory. The effect of solvent (DMSO) was included using the integral equation formalism for the polarizable continuum model (IEFPCM) on Gaussian 03W [27].

The conformational behavior of each conformer was studied by semiempirical calculations using the PM3 method. Scanning of 360° in the dihedral angle N2—C10—C11—C12 was performed with an increment of 1° with full optimization at each step.

A geometry optimization was performed on the dimer and chain crystal structures of compound **4**, based on the experimental crystal structure after refinement. The calculations were performed within the framework of DFT using CASTEP program of Materials Studio software [28]. The electronic structure was calculated by optimizing all the atoms of the crystal using ultrasoft pseudopotentials within a plane wave basis with cutoff energy of 340 eV. The generalized gradient approximation (GGA) were applied using the Perdew–Burke–Ernzerhof (PBE) exchange–correlation functional [29]. The energy tolerance, the maximum force tolerance and the maximum displacement tolerance were 1.0×10^{-5} eV/atom, 0.03 eV/Å and 0.001 Å, respectively.

Acknowledgements

The use of the EPSRC X-ray crystallographic service at Southampton and the valuable assistance of the staff there are gratefully acknowledged. J.L.W. thanks CAPES for financial support. E.B.L. thanks CAPES for master scholarship. J.D.Y. thanks FAPERJ for financial support. Prof. Peter Rudolf Seidl (UFRJ) is thanked for the use of the Materials Studio package.

Appendix A. Supplementary material

Full details of the crystal structure determinations in cif format are available in the online version, at doi: (to be inserted) and have also been deposited with the Cambridge Crystallographic Data Centre with deposition numbers 895995 (compound **3**), 895997 (compound **1**), 895998 (compound **4**) and 895999 (compound **2**). Copies of these last can be obtained free of charge on written application to CCDC, 12 Union Road, Cambridge, CB2 1EZ, UK (Fax: +44 1223 336033); on request by email to deposit@ccdc.cam.ac.uk or by access to http://www.ccdc.cam.ac.uk. Supplementary data associated with this article can be found, in the online version, at http://dx.doi.org/10.1016/j.molstruc.2012.09.058.

References

[1] S.A. Carvalho, W.T.A. Harrison, C.A.M. Fraga, E.F. da Silva, J.L. Wardell, S.M.S.V. Wardell, Z. Kristallogr. 224 (2009) 598–606;
R.A. Howie, M.V.N. de Souza, M. de L. Ferreira, C.R. Kaiser, J.L. Wardell, S.M.S.V. Wardell, Z. Kristallogr. 225 (2010) 440–447;
C. Glidewell, J.N. Low, J.M.S. Skakle, J.L. Wardell, Acta Crystallogr. C 59 (2003) o-98–o-101;
C. Glidewell, J.N. Low, J.M.S. Skakle, J.L. Wardell, Acta Crystallogr. C 60 (2004) o-19–o-23;
J.L. Wardell, J.M.S. Skakle, J.N. Low, C. Glidewell, Acta Crystallogr. C 61 (2005) o-10–o-14;
G. Ferguson, C. Glidewell, J.N. Low, J.M.S. Skakle, J.L. Wardell, Acta Crystallogr. C 61 (2005) o-613–o-616.

[2] A.F. Nogueira, T.R.A. Vasconcelos, J.L. Wardell, S.M.S.V. Wardell, Z. Kristallogr. 226 (2011) 846–860.

[3] A.F. Nogueira, E.C. Azevedo, V.F. Ferreira, A.J. Araújo, E.A. dos Santos, C. Pessoa, L.V. Costa-Lotufo, R.C. Montenegro, M.O. de Moraes, T.R.A. Vasconcelos, Lett. Drug Des. Disc. 7 (2010) 551–555.

[4] I. Caleta, M. Kralj, M. Marjanovic, B. Bertosa, S. Tomic, G. Pavilovic, K. Pavelic, G. Karminski-Zamola, J. Med. Chem. 52 (2009) 1744–1756.

[5] A. Rana, N. Siddiqui, S.A. Khan, Ind. J. Pharm. Sci. 69 (2007) 10–17.
[6] M. Ban, H. Tagushi, T. Katsushima, M. Takahashi, K. Shinoda, A. Watanabe, T. Tominaga, Bioorg. Med. Chem. 6 (1998) 1069–1076.
[7] M. Yoshida, N. Hayakawa, N. Hayashi, T. Agatsuma, Y. Oda, F. Tanzawa, S. Iwasaki, K. Koyama, H. Furukawa, S. Kurakata, Bioorg. Med. Chem. Lett. 15 (2005) 3328–3332.
[8] T.D. Bradshaw, A.D. Westwell, Curr. Med. Chem. 11 (2004) 1009–1021 (and earlier papers).
[9] J. Easmon, G. Heinisch, J. Hofmann, T. Langer, H.H. Grunicke, J. Fink, G. Pürstinger, Eur. J. Med. Chem. 32 (1997) 397–408.
[10] S.M. Westway, M. Thompson, H.K. Rami, G. Stemp, L.S. Trouw, D.J. Mitchell, J.T. Seal, S.J. Medhurst, S.C. Lappin, J. Biggs, J. Wright, S. Arpino, J.C. Jerman, J.E. Cryan, V. Holland, K.Y. Winborn, T. Coleman, A.J. Stevens, J.B. Davis, M.J. Gunthorpe, Bioorg. Med. Chem. Lett. 18 (2008) 5609–5613.
[11] V. Sharma, K.V. Sharma, Eur. J. Chem. 6 (2009) 348–356;
I. Sigmundová, P. Zahradnik, P. Magdolen, H. Bujdakova, Arkivoc 8 (2008) 183–192.
[12] J.L. Wong, M.F. Zady, J. Org. Chem. 40 (1975) 2512–2516.
[13] V.A. Bren, V.I. Minkin, E.N. Shepelenko, A.D. Dobonoso, A. Ya Bushkov, Mendeleev Commun. 1 (1991) 72–73;
S.K. Dey, T.S.M. Abedin, L.N. Dawe, S.S. Tandon, J.L. Collins, L.K. Thompson, A.V. Postnikov, M.S. Alam, P. Muller, Inorg. Chem. 46 (2007) 7767–7781;
I.G. Pervova, S.A. Melkozerov, P.A. Slepukhin, G.N. Lipunova, V.A. Barachevskii, I.N. Lipunov, Russ. J. Gen. Chem. 80 (2010) 987–993.
[14] C.Z. Chen, F.X. Huang, Y.Q. Wu, D.H. Gu, F.X. Gan, Inorg. Chem. Commun. 9 (2006) 21–24;
C.Z. Chen, Y.Q. Wu, D.H. Gu, F.X. Gan, Spectrochim. Acta Part A Mol. Biomol. Spectrosc. 68 (2007) 918–926.
[15] K. Usegi, L.J. Sik, H. Nishioka, T. Kumagai, T. Nagahiro, Microchem. J. 50 (1994) 88–93;
T. Odashima, H. Ishii, Bunseki Kagaku 31 (1982) 343–345.
[16] D.S. Deshpande, Curr. Sci. 46 (1977) 97–99.
[17] I.G. Pervova, S.A. Melkozerov, P.A. Slepukhin, G.N. Lipunova, V.A. Barachevskii, I.N. Lipunov, Russ. J. Gen. Chem. 80 (2010) 987–993.
[18] S. Kwon, M. Tanaka, K. Isagawa, Nippon Kagaku Kaishi (1973) 1314–1319.
[19] J. Bernstein, R.E. Davis, L. Shimoni, N.-L. Chang, Angew. Chem. Int. Ed. Engl. 34 (1995) 1555–1573.
[20] A.L. Spek, J. Appl. Crystallogr. 36 (2003) 7–13.
[21] MERCURY 2.3, Cambridge Crystallographic Data Centre.
[22] R.W.W. Hooft, COLLECT, Data Collection Software, Nonius BV, Delft, The Netherlands, 1998.
[23] Z. Otwinowski, W. Minor, Processing of X-ray diffraction data collected in oscillation mode, in: C.W. Carter, Jr., R.M. Sweet (Eds.), Macromolecular Crystallography, Part A. Methods in Enzymology, vol. 276, Academic Press, New York, pp. 307–326, 1997.
[24] G.M. Sheldrick, SADABS, Version 2.10, Bruker AXS Inc., Madison, Wisconsin, USA, 2003.
[25] L.J. Farrugia, J. Appl. Crystallogr. 3 (1999) 837.
[26] G.M. Sheldrick, Acta Crystallogr. A64 (2008) 112–122.
[27] M.J. Frisch, G.W. Trucks, H.B. Schlegel, G.E. Scuseria, M.A. Robb, J.R. Cheeseman, J.A. Montgomery, Jr., T. Vreven, K.N. Kudin, J.C. Burant, J. M. Millam, S.S. Iyengar, J. Tomasi, V. Barone, B. Mennucci, M. Cossi, G. Scalmani, N. Rega, G.A. Petersson, H. Nakatsuji, M. Hada, M. Ehara, K. Toyota, R. Fukuda, J. Hasegawa, M. Ishida, T. Nakajima, Y. Honda, O. Kitao, H. Nakai, M. Klene, X. Li, J.E. Knox, H.P. Hratchian, J.B. Cross. C. Adamo, J. Jaramillo, R. Gomperts, R.E. Stratmann, O. Yazyev, A.J. Austin, R. Cammi, C. Pomelli, J.W. Ochterski, P.Y. Ayala, K. Morokuma, G.A. Voth, P. Salvador, J.J. Dannenberg, V.G. Zakrzewski, S. Dapprich, A.D. Daniels, M.C. Strain, O. Farkas, D.K. Malick, A.D. Rabuck, K. Raghavachari, J.B. Foresman, J.V. Ortiz, Q. Cui, A.G. Baboul, S. Clifford, J. Cioslowski, B.B. Stefanov, G. Liu, A. Liashenko, P. Piskorz, I. Komaromi, R.L. Martin, D.J. Fox, T. Keith, M.A. Al-Laham, C.Y. Peng, A. Nanayakkara, M. Challacombe, P.M.W. Gill, B. Johnson, W. Chen, M.W. Wong, C. Gonzalez, J.A. Pople, Gaussian 03, Revision C.01, Gaussian, Inc., Wallingford, CT, USA, 2004.
[28] Accelrys, Materials Studio CASTEP, Accelrys, San Diego, 2011.
[29] J.P. Perdew, K. Burke, M. Ernzerhof, Phys. Rev. Lett. 77 (1996) 3865–3868.